REMARKS/ARGUMENTS

The Amendment:

The specification has been amended on pages 4 and 5 to correct the spelling of "granular" and to add matter which was inadvertently omitted from this continuation application. The amended sentence was obviously incorrect and the correct version of this sentence appears in lines 21-23 of page 5 of the parent application, Ser. No. 09/9090,066.

The claims have been amended to recite that a selected surface of the polyethylene object is coated and that heat is applied locally to the coated, selected surface. Support for the amendment appears on page 2, line 14 and page 5, lines 7-10.

The Invention:

Applicants' invention is a method for imparting a permanently roughened surface to a polyethylene object, Coatings do not readily adhere to polyethylene, which is the most resistant to coatings of all the polyolefins. Applicants have achieved permanent modification of the surface of even polyethylene by a method in which a coating of polyethylene powder admixed with inorganic particles is fused into the surface of a polyethylene object. The method requires localized, radiant heating of the coated surface of the object sufficiently to melt both the coating and the surface of the object to fuse the coating into the surface of the object.

The Rejections:

Claims 1, 4, 6, 9 and 10 are rejected as unpatentable under 35 U.S.C.§103 in view of the teachings of Jenett and Hoopman et al.

Claims 5, 7, 11 and 12 are rejected as unpatentable under 35 U.S.C.§103 in view of the teachings of Jenett, Hoopman et al and Brant et al..

Claims 5, 7, 11 and 12 are rejected as unpatentable under 35 U.S.C.§103 in view of the teachings of Jenett, Hoopman et al and Kagota et al.

The References:

Jenett coats the surface of a plastic object with a dispersion of polyethylene powder in a liquid mixture of a solvent (xylene) and non-solvent (petroleum naphtha). The polyethylene powder has a fusing temperature below that of the plastic object and a lower molecular weight than the plastic of the object (col. 3, lines 50-55).

The coated plastic object is then placed in an oven (see the examples) and heated to a temperature above the softening or fusing temperature of the polyethylene powder in the coating, but below the softening point of the base (plastic object) for sufficient time to evaporate the

solvents (col. 4, lines 65) and form the coating into a film (col. 4, lines 66-68). The heating is insufficient to cause melting of the base, and must be from 80° C. to 5° C. below the melting point of the surface; claim 3, lines 32-36 and col. 5, lines 39-41. Since the coated object is placed in an oven and heated, the entire object is unavoidably heated to the oven temperature.

Jenett states that the heating should raise the coating to an elevated temperature below the softening point of the base to fuse and level the polyethylene coating and form a homogeneous film (col. 2, lines 24-28). Jenett restates this at col. 4, lines 63-64, as: heating at an elevated temperature: "....below the softening point of the base..."

This reference is replete with specific instructions to those skilled in the art that the heat treatment should not cause melting of the base (coated object).

Jenett discloses that a modified phenol formaldehyde type resin or rubber resin can be included in the polyethylene powder dispersion to add tack (col. 5, lines 12-15). Phenol formaldehyde resins and rubber are thermosetting resins and do not melt when heated . These resins, therefore, can not fuse into the polyethylene object at any temperature.

Hoopman et al disclose coating a backing sheet with a mixture of inorganic particles in a glue. The inorganic solids are dispersed in the glue which is adhesively bonded to the backing sheet; with an interface between the surface 11 of the backing sheet and the layer of glue and abrasive composites 15; see Fig. 10. Also see Fig. 2 and note the interface line between the continuous land layer 27 of the glue and abrasive composite material and the backing 26. As in Jenett, the glue used by Hoopman et al is a thermosetting resin; col. 12, lines 24-62 cured by heat and/or a cationic or free radical agent. Hoopman et al cure the coating by applying an "energy source" to the coated sheet. The energy source can be ionizing radiation for free radical catalyzed cures, or thermal energy to heat the coated sheet to a temperature range from about 30° to 150°C. for 5 minutes to 24 hours (col. 20, lines 28-53).

Brant et al disclose a cling film which is extruded from a melt of a hydrocarbon resin tackifier and a copolymer of ethylene and a C_3 to C_{12} olefin comonomer. This film may be co-extruded with a polypropylene slip layer. There is no suggestion that a tackifier which functions in the prior art to impart a cling property to a dry film would be functional as a tackifier for a liquid coating, nor is there any suggestion in Jenett that such a tackifier would be of any benefit in the Jenett coating.

Kagota et al teaches that an aqueous suspension of polyethylene and a tackifier is useful as an adhesive. This patent, however, teaches that it is necessary to incorporate hydrophilic groups, i.e., carboxyl groups, in the polyethylene; see column 3, lines 32-52. Kagota et al do not

apply the aqueous adhesive to a preformed plastic object. Instead, the adhesive is coated onto a label, the label is heated and the hot label is applied to a polypropylene bottle. Again, as with Hoopman et al and Brandt et al, there is no teaching which cures the defect in Jenett, i.e., the explicit teaching that the coated surface must not be melted, and without melting this surface, one can not achieve fusion of the coating into the surface.

Applicants' Arguments:

The Jenett patent is a classic instance of a prior art reference which teaches away from the claimed invention. Those skilled in the art are instructed in unambiguous terms to avoid heating of the Jenett coating to a temperature which will cause melting of the base. These teachings have been cited, *supra*, in the discussion of the Jenett patent. Where a reference warns against the practice of the claimed invention, one skilled in the art cannot be expected to combine it with another teaching; see *In re Fine*, 837 F.2d 1071, 5 USPQ2d 1569 (Fed. Cir. 1988) and *In re Gurley*, 27 F.2d 551, 31 USPQ2d 1130 (Fed. Cir. 1993). A teaching away from the claimed invention directs one skilled in the art in a path divergent from that taken by applicants. Jenett clearly meets this standard by its teaching that one must avoid melting the base. There is no need to infer a meaning or to read between the lines to understand what Jenett teaches. The teaching is crystal clear; do not heat the coated article sufficiently to cause melting of the base.

The examiner has argued that polymers do not have a sharp melting temperature, but instead melt over a temperature range and, therefore: (1) Jenett actually contemplates reaching a melt condition of the coated base, or (2) those skilled in the art would obviously conclude that some melting must occur. This is an unwarranted interpretation of the reference. Note that Jenett does not refer to a melting <u>temperature</u> of the surface (base). Instead the patent states that the heating must be below the softening <u>point</u> of the surface and below the melting <u>point</u> of the surface. It is the condition of <u>melting</u> of the surface which must be avoided, not some arbitrary temperature.

Attached hereto is a copy of *Structure and Mechanical Properties Of Ultra-High Molecular Weight Polyethylene Deformed Near Melting Temperature*; International Union of Pure and Applied Chemistry, ©1991 IUPAC, p. 1794-1804. A differential scanning calorimeter (DSC) graph for the heating and cooling cycles of UHMWPE polyethylene are shown and a table of melting temperatures of three grades of the polymer are presented on page 1796. The following temperatures are identified: onset melt temperature; peak melt temperature; and end melt temperature.

Also attached is a copy of *Characterization of Polyethylene with Differential Scanning Calorimetry (DSC) and Dynamic Mechanical Analysis (DMA)* Netzsch Applications Laboratory Newsletter, p. 1-11. This article presents DSC graphs for 4 categories of polyethylene; ultrahigh molecular weight, high density; low density and linear low density polyethylene on pages 6-8, evidencing that all grades of polyethylene have a characteristic sharp melting point range with onset, peak and end melt temperatures, such as those shown in the IUPAC article..

What is significant from these articles is that there is no single melt temperature for polyethylene. There is a peak temperature of melting and there are onset and end melt temperatures. However, Jenett doesn't refer to any melting temperature. Instead, Jenett refers to melting point. That melting point is reached at the onset melt temperature and Jenett teaches that one must stay below that onset melting temperature. This teaching is clear, unambiguous and directs those skilled in the art away from the claimed invention.

The secondary references to not suggest any heat treatment which is contrary to that taught by Jenett. There is no suggestion by Hoopman et al that the coated backing sheet should be heated to melt the backing sheet.. As in Jenett, the thermosetting resins used by Hoopman et al can not melt and can not fuse into the coated sheet even if one attempted to melt the backing sheet.

Brand et al disclose the formation of a cling film which is extruded or co-extruded and there is no suggestion of coating a preformed film and heating of a coated preformed film.

Kogota et al lacks a teaching of applying a coating to a plastic object and heating the coated surface of the object. As with Hoopman et al and Brandt et al, there is no teaching which cures the defect in Jenett, i.e., the failure to disclose heating of a coated surface to the melt temperature of the coated article to achieve fusion of the coating into the surface.

The claims are believed to be of proper form and scope and for the reasons set forth herein, define a patentable invention over the prior art. Examination and allowance are solicited.

Respectfully submitted.

Robert E. Strauss

928 717-9924

INTERNATIONAL UNION OF PURE AND APPLIED CHEMISTRY

MACROMOLECULAR DIVISION
COMMISSION ON POLYMER CHARACTERIZATION AND PROPERTIES
WORKING PARTY ON STRUCTURE AND PROPERTIES OF COMMERCIAL POLYMERS*

STRUCTURE AND MECHANICAL PROPERTIES OF ULTRA-HIGH MOLECULAR WEIGHT POLYETHYLENE DEFORMED NEAR MELTING TEMPERATURE

(Technical Report)

Prepared for publication by

K. NAKAYAMA[1], A. FURUMIYA[2], T. OKAMOTO[2], K. YAGI[2], A. KAITO[1], C. R. CHOE[3],
L. WU[4], G. ZHANG[4], L. XIU[4], D. LIU[4], T. MASUDA[5], A. NAKAJIMA[6]

[1]Research Institute for Polymers and Textiles, 1-1-4 Higashi, Tsukuba, Ibaraki 305, Japan
[2]Mitsui Petrochemical Co., Ltd., 3-2-5, Kasumigaseki, Chiyoda-ku, Tokyo 100, Japan
[3]Korea Institute of Science and Technology, P.O. Box 131, Cheongryang, Seoul, Korea
[4]Testing Center of Textile Academy China, P.O. Box 651, Beijing, China
[5]Research Center for Biomedical Engineering, Kyoto University, Kyoto 606, Japan
[6]Osaka Institute of Technology, 5-16-1 Ohmiya, Asahi-ku, Osaka 535, Japan

for the East Asia Sub-Group

Chairman: A. Nakajima; *Secretary*: T. Masuda; *Members*: J. H. Byon; C. R. Choe; T. Hayashi; M. Hirami; M. Isshi; B. Jiang; J. C. Jung; C. K. Kim; C. Y. Kim; K. U. Kim; S. C. Kim; H. Kodama; Y. Kometani; H. Kondo; Y. Kubouchi; J. Li; N. Nagata; K. Nakayama; T. Ohmae; T. Okamoto; R. Qian; K. Sakamoto; S. Shimotsuma; S. Suzuki; S. Tsuchiya; L. Wu; J. K. Yeo; A. Yoshioka

Structure and mechanical properties of ultra-high molecular weight polyethylene deformed near melting temperature

ABSTRACT: Some physical properties of ultra-high molecular weight poly-ethylene (UHMWPE) were studied in regard to its molecular weight. The main samples employed in this work were three grades of commercially available UHMWPE. UHMWPE is known as a high performance linear poly-ethylene with excellent physical properties. Owing to its high molecular weight and the presence of entanglements of molecular chains, UHMWPE has very high melt viscosity. The object of this report is to investigate the effect of molecular weight on microstructure and mechanical properties of UHMWPE. Following items are discussed: powder properties of UHMWPE, relationship between properties and molecular weight, and drawabilities at various temperatures. The characteristic features are higher drawability of UHMWPE in the molten state and high tensile moduli of hot drawn sheets. Structure of hot drawn UHMWPE sheets was also discussed.

INTRODUCTION

High density polyethylene (HDPE) is one of the mass production commodity polymers. In general, HDPE is prepared by solution, slurry, and gas-phase polymerization. Slurry poly-merization is a widely used method because of possibility of producing wide range of commer-cial grades including ultra-high molecular weight polyethylene (UHMWPE). UHMWPE is a linear polyethylene with molecular weights over 1×10^6 and is known as a high performance poly-mer with excellent physical properties, such as high toughness, self-lubrication, and abra-sion-resistance. Owing to its high molecular weight and the presence of entanglements of molecular chains, UHMWPE has very high melt viscosity and does not flow like usual poly-ethylene.

In spite of its poor processibility, UHMWPE is widely used for various applications. Mitsui Petrochemical Industries has been manufactur-ing UHMWPE. The Sub-Group meeting in East Asia of IUPAC Working Party IV-2-1 has worked to investigate the relationships between molecular weight and physical properties of commercial UHMWPE. This report also describes the drawability of UHMWPE in the molten state and the structure and properties of drawn sheets.

MATERIALS USED AND MOLECULAR CHARACTERISTICS

The samples employed in this report were three grades of ultra-high molecular weight polyeth-ylene (UHMWPE), Hizex Million 145M, 240M, and 340M. Different grades of high-density poly-ethylene (HDPE) and UHMWPE were also used for comparisons. These polyethylene samples were manufactured by Mitsui Petrochemical Indus-tries. Their molecular characteristics are given in Table 1. Although equations repre-senting the relationship between intrinsic viscosities and molecular weights in the molecular weight region of general-purpose polyethylenes have been proposed by R. Chiang (ref. 1) and P. M. Henry (ref. 2), there is

TABLE 1. Molecular characteristics of polyethylene samples

Sample	Intrinsic Viscosity $[\eta](dl/g)$	Molecular Weight $M_v \times 10^{-4}$
PE- 1	1.21	7.0
PE- 2	1.46	9.0
PE- 3	1.84	12.4
PE- 4	2.14	15.2
PE- 5	2.73	21.3
PE- 6	2.93	23.4
PE- 7	3.23	26.8
PE- 8	3.47	29.5
PE- 9	7.80	89.5
PE-10	11.3	148
PE-11	12.2	165
PE-12	16.8	256
PE-13	20.7	341
PE-14	25.6	456
PE-15	30.5	580
PE-16	31.4	603

$[\eta]$: at 135 °C, in decahydronaphthalene

practically no formula proposed for the ultrahigh molecular weight polyethylenes. The only equation ever introduced is the one provided in ASTM D4020 for the relationship between nominal molecular weights and intrinsic viscosities for polyethylenes having reduced viscosities higher than 2.3, which is based on weight average molecular weights. In order to ensure accuracy, it would be more appropriate to discuss the particular relationship in terms of intrinsic viscosities. In our discussion here, however, for the sake of convenience, the molecular weights of all polyethylene samples were converted into the nominal molecular weights, M_v by use of the equation given in ASTM D 4020.

$$M_v = 5.37 \times 10^4 [\eta]^{1.37} \tag{1}$$

The intrinsic viscosities $[\eta]$ were measured in decahydronaphthalene at 135 °C. Commercially available Hizex Million 145M, 240M and 340M correspond to PE-9, PE-12 and PE-14 shown in Table 1, respectively.

POWDER PROPERTIES

UHMWPE is produced by a slurry process and supplied as a fine powder. It is well known that the properties of polymer powder affect the processibility (ref. 3). UHMWPE powders from different suppliers have different powder characteristics (ref. 4). The powder morphologies and thermal properties of the three grades of UHMWPE will be discussed below.

Morphology

The bulk density of three UHMWPE powders was approximately 0.45 g/cm^3. The morphology of as-polymerized powder was observed by using a scanning electron microscope (SEM), Hitachi S-800. Fig. 1 shows SEM micrographs of the 240 M powder. The particle diameter is in the order of 200 μm. The secondary particle consists of primary particles. A close observation reveals surface texture of the primary particle.
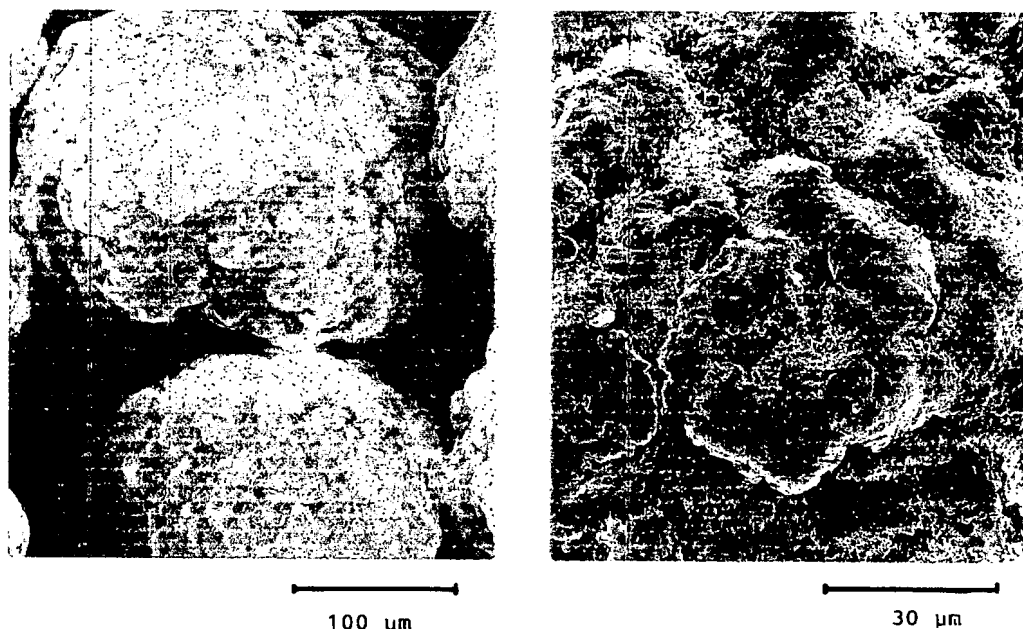

|◄━━━━━━━━━━►|
100 μm

|◄━━━━━━━━━━►|
30 μm

Figure 1. Powder morphology of UHMWPE.

Thermal properties

The melting and crystallization temperatures of powder samples were determined by differential scanning calorimeter (DSC), Seiko DSC 210, calibrated with a melt transition of Indium. Fig. 2 shows the DSC curves of 240 M powder sample. The first and second thermal cycles by heating the sample at a rate of 10 °C/min in nitrogen were recorded. The extrapolated onset, peak and extrapolated end temperatures for melting and crystallization are shown in Table 2. It is seen that the melting temperatures of as-polymerized UHMWPE powders lie in a range of 140 to 143 °C. After the first thermal cycle, the melting temperature decreased by 8 - 10 °C. The peak melting temperature of UHMWPE increases with increasing molecular weight.
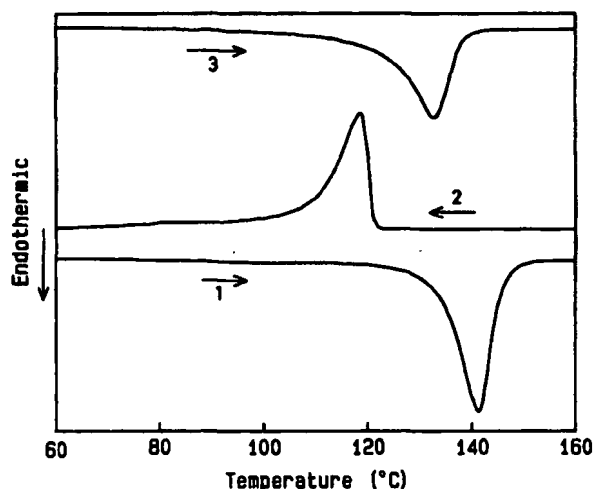
Figure 2. DSC curves for
UHMWPE 240 M powder:
1;first heating process,
2;cooling process,
3;second heating process.

TABLE 2. Melting and crystallization temperatures of UHMWPE powder
samples

Powder	First scanning						Second scanning		
	T_{im}	T_{pm}	T_{em}	T_{ic}	T_{pc}	T_{ec}	T_{im}	T_{pm}	T_{em}
					(°C)				
145 M	130.7	140.2	147.5	118.9	116.7	107.7	121.7	132.9	139.4
240 M	132.8	141.2	146.3	120.6	118.2	108.2	120.6	132.9	138.1
340 M	135.0	143.1	148.1	121.9	119.1	109.9	125.2	134.4	139.2

T_{im} : extrapolated onset temperature of melting
T_{pm} : melting peak temperature
T_{em} : extrapolated end temperature of melting
T_{ic} : extrapolated onset temperature of crystallization
T_{pc} : crystallization peak temperature
T_{ec} : extrapolated end temperature of crystallization

PROPERTIES–MOLECULAR WEIGHT RELATIONSHIPS

Chemically, UHMWPE is identical with HDPE. In general, the molecular weight strongly influ-
ences on physical properties of polymers. Attempts have been made to deal with the rela-
tionships between physical properties and molecular weights of UHMWPE.

Preparation of specimen

The sheets of thickness 1 – 3 mm were
prepared by compression molding of UHMWPE
powders with a cylindrical type mold. The
molding procedures to get homogeneous and
uniform specimens are shown in Table 3.
The powder was placed in the mold, heated
and kept under a pressure of 10 MPa.
Pressure applied on the melt was then
decreased to 5 MPa. After the dwell-time
of 20 minutes, the sample was cooled, kept
at 20 – 30 °C under a pressure of 20 MPa
and then taken out of the mold.

TABLE 3 Condition for compression molding
of UHMWPE

Step	Temperature (°C)	Pressure (MPa)	Hold time (min)
1st	200 – 220	10	5
2nd	200 – 220	5	15
3rd	20 – 30	5	0.5
4th	20 – 30	20	20

TABLE 4   General properties of polyethylene

Samples	Molecular Weight $M_v \times 10^{-4}$	Density $d(g/cm^3)$	Vicat softening temperature (°C)	Shore hardness (D scale)
PE- 1	7.0	0.962	122	68
PE- 2	9.0	0.964	124	68
PE- 3	12.4	0.953	125	64
PE- 4	15.2	0.956	126	64
PE- 5	21.3	0.948	120	61
PE- 6	23.4	0.955	124	64
PE- 7	26.8	0.955	122	63
PE- 8	29.5	0.954	126	65
PE- 9	89.5	0.942	129	65
PE-10	148	0.947	131	65
PE-11	165	0.947	130	65
PE-12	256	0.935	132	63
PE-13	341	0.938	134	66
PE-14	456	0.932	134	65
PE-15	580	0.931	134	65
PE-16	603	0.931	135	66

General properties

Some physical properties of polyethylene tested are shown in Table 4. The densities of polyethylene sheets are in a range of 0.931 - 0.964 g/cm³ and depend on the molecular weight. In the case of HDPE, with increasing molecular weight, the crystallinity decreases. UHMWPE has relatively low densities.

The softening temperature and hardness are the bases of general properties and important in the end-uses of PE. The Vicat softening temperature is generally used for judging the use-limitations at high temperature. As is understood from Table 4, UHMWPE shows higher heat resistance.

The measurement of Shore hardness was conducted by the use of a type D durometer hardness tester. The scale of hardness was read after the load had been applied on the indenter for 5 s. As shown in Table 4, it is difficult to discuss the exact relationship between the hardness and molecular weight of polyethylene.

The abrasion-resistance of polyethylene sheet was evaluated by the sand abrasion method. Test pieces 75 mm × 25 mm × 6 mmt were rotated at 1500 r.p.m. in a sand slurry bath (8 kg of standard sand and 6 kg of water). After the rotation for 20 hrs, the weight loss of specimen sheet was measured. The loss weight is plotted against molecular weight in Fig. 3. Loss weight decreases with increasing molecular weight. The rate of increase of abrasion-resistance with molecular weight is very high at first and finally levels off. The long molecular chain of UHMWPE confers the excellent abrasion-resistance.

Mechanical properties

Mechanical characteristics of polymers are related to molecular weight, crystallinity, orientation, morphological structure and other parameters. Attempts have been made to summarize the mechanical data and correlate mechanical properties to the molecular weight of polyethylene.

The stiffness or relative flexibility of HDPE and UHMWPE was evaluated. The apparent bending modulus of the specimen cut from molded sheet was measured with a cantilever beam testing apparatus, Olsen stiffness tester, in accordance with ASTM D747. The dependence of stiffness on the molecular weight was shown in Fig. 4. Clearly, stiffness decreases with increasing molecular weight.

The long molecular chain of UHMWPE results in high impact toughness. The resistance to breakage by flexural shock of specimen was measured by means of the IZOD and Dynstat tests at room temperature. The effect of molecular weight on the impact strength is shown in Fig. 5. The results of IZOD test are nearly equal to those of Dynstat test. UHMWPE shows an excellent mechanical endurance. An increase in molecular weight is accompanied with an increase in the impact strength and a maximum is exhibited in the region of molecular weight of 1×10^6 and 2×10^6. In general, an increase in average molecular weight of HDPE leads

to increase in impact strength, but this is
achieved when the long-chain molecules are
mixed with each other. The impact strength
of the UHMWPE of $M_v > 2 \times 10^6$ decreases with
increasing molecular weight. This suggests
that powder grain boundaries remain in
compression molded sheets of higher molecu-
lar weight polymer.

The stress-strain measurements were carried
out. As shown in Fig. 6, the yield strength
of polyethylene decreases monotonically with
the molecular weight. The breaking strength
rises sharply and polyethylenes of $M_v >$
2×10^5 exhibit higher breaking strengths.
When strain at break is plotted against the
molecular weight, a maximum appears
(Fig. 7). This reduction of elongation at
break of higher molecular weight polymers
may relate to the powder grain boundaries in
compression molded sheets.
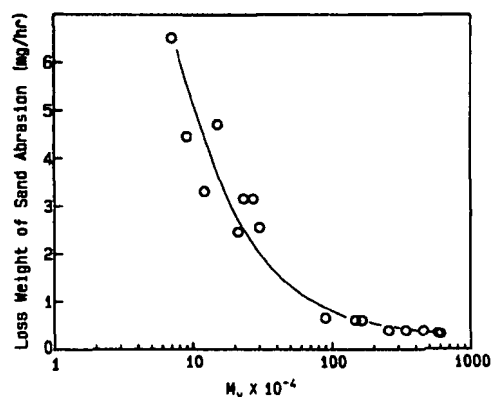
Figure 3. Abrasion-resistance vs. molecular
weight for polyethylene samples.
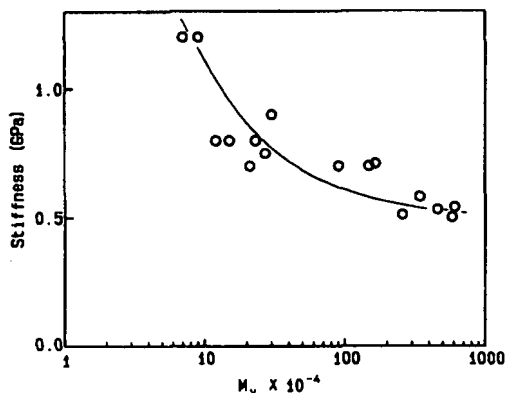
Figure 4. Olsen stiffness vs. molecular
weight for polyethylene samples.
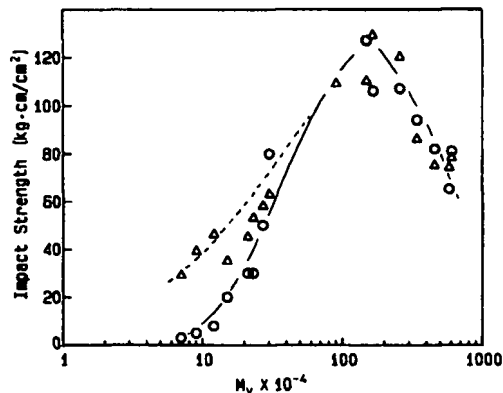
Figure 5. Impact strength vs. molecular
weight for polyethylene samples:
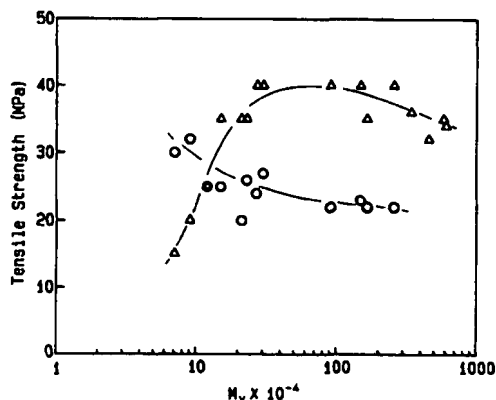O ;IZOD impact strength,
△ ;Dynstat impact strength.

Figure 6. Tensile strength vs. molecular
weight for polyethylene samples:
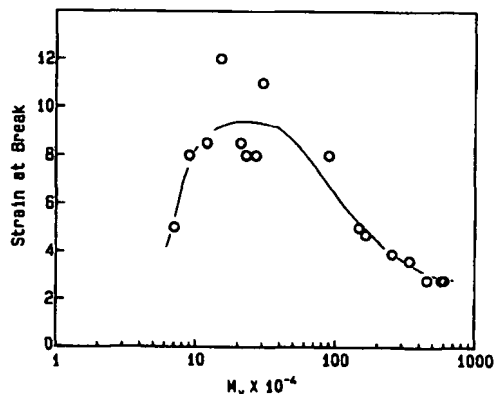O ;Yield stress, △ ;Tensile stress at break.

Figure 7. Elongation at break vs.
molecular weight for polyethylene samples.

DRAWABILITY OF UHMWPE

The effect of molecular weight on the drawing behavior of linear polyethylene was discussed by Capaccio et al. (ref.5,6) and it was shown that the draw ratio obtainable depended on the molecular weight characteristics of polymer and the crystallization procedures. However, UHMWPE having an excellent physical properties exhibits very high melt viscosity, which may limit its processibility. Here we summarize the drawabilities of three grades of UHMWPE at various temperatures.

Fig. 8 shows the stress - strain curves of 240 M sheet measured at various temperatures for a sample 40 mm in length and at a tensile rate of 50 mm/min. The UHMWPE sheet is able to be stretched even in the molten state. The yield points are observed in the stress - strain curves of melt drawing and solid drawing processes. The strain at yield point for melt drawing is higher than that for solid drawing. The tensile stress for melt drawing is much lower than that for solid drawing.

It is important to consider the presence of a superstructure network formed by entanglement of molecular chains. Owing to the presence of entanglements of molecular chains, the UHMWPE loses fluidity and shows rubber-like elasticity in the melt. In the course of melt drawing, the entanglement plays the role as transmitter of drawing force and the molecular chains supported by the entanglement orient in the stretching direction. This is why the UHMWPE can be stretched in the molten state.

Figs. 9 and 10, respectively, show the temperature dependencies of the initial tensile modulus and of yield stress for UHMWPE. The initial tensile modulus and yield stress gradually decrease with increasing temperature in the solid state and sharply fall off at the melting temperature of UHMWPE. In the solid state, the initial tensile modulus and yield stress are not affected significantly by molecular weight, whereas the tensile properties in the molten state are very sensitive to molecular weight of UHMWPE. As the density of chain entanglements increases with molecular weight, the higher modulus of elasticity is obtained at higher molecular weight in the molten state.

Fig. 11 shows the maximum draw ratio of two grades of UHMWPE as a function of temperature. The maximum draw ratio increases with increasing drawing temperature. The maximum draw ratio for melt drawing is more than twice as large as that for the solid drawing, suggesting that the melt drawing is effective for stretching UHMWPE. At a given temperature, the maximum draw ratio of UHMWPE decreases with increasing molecular weight.

According to the theory of rubber elasticity (ref. 7), the maximum draw ratio of polyethylene is as low as 3.7 (ref. 8), if the entanglements of molecular chains are completely trapped and act as permanent crosslinks during the drawing. As the disentanglement is restricted in lower temperatures, the UHMWPE sheet shows lower extensibility than the normal molecular weight HDPE in the solid state. On the other hand, in the molten state, one can expect the disentanglement of molecular chains through slippage, which makes it possible to stretch the UHMWPE to a higher extension.
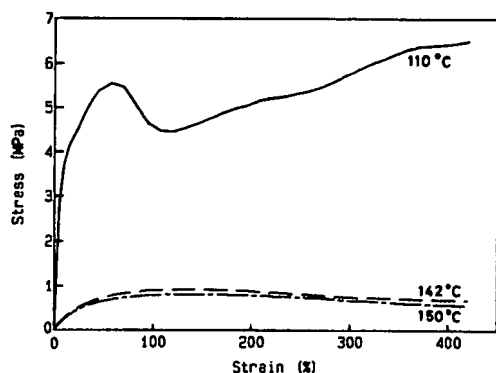

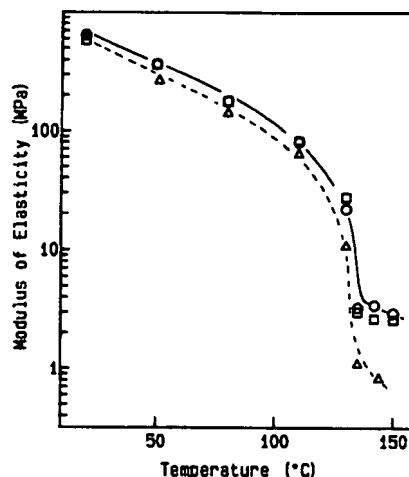Figure 8. Stress - strain curves at 110, 142, and 150 °C for 240 M sheet.

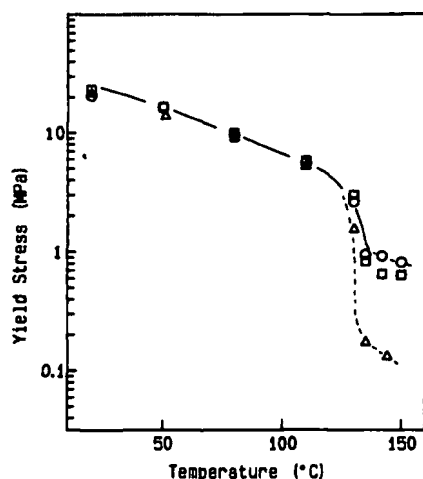Figure 9. Temperature dependence of initial tensile modulus: $\triangle$;145 M, $\bigcirc$;240 M, $\square$;340 M.

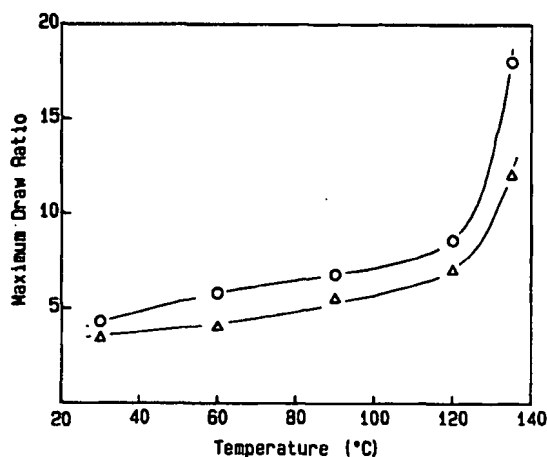Figure 10. Temperature dependence of yield stress: △;145 M, ○;240 M, □;340 M

Figure 11. Maximum draw ratio vs. temperature: ○;240 M, △;340 M

TENSILE PROPERTIES OF HOT DRAWN UHMWPE

Here we summarize the tensile properties of hot drawn UHMWPE sheets. Three grades of UHMWPE samples were used and the uniaxial drawing was conducted in the solid and the molten states. The effects of drawing temperature, drawing ratio, and molecular weight on the tensile properties were investigated.

Strips with gauge dimension of 2 × 2 cm were uniaxially drawn in the solid state (120-130 °C) and in the molten state (135-150 °C). Tensile properties were measured at 23 °C and a relative humidity of 50 %, with a gauge length of 16 mm and a tensile rate of 4 mm/min.

Figs. 12 and 13 show the Young's modulus and tensile strength, respectively, of hot drawn 145 M sheets. The Young's modulus and tensile strength increase monotonically with increasing draw ratio. The increase of the Young's modulus is quite appreciable in the higher draw ratio range. The Young's modulus and tensile strength are improved more efficiently by solid drawing than by melt drawing. Although the 145 M sheet can be melt drawn at a draw ratio as high as 36 at 135 °C, its Young's modulus and tensile strength are much lower than those obtained by solid drawing.

Figs. 14 and 15 show the Young's modulus and tensile strength, respectively, of the 240 M sheet. The Young's modulus and tensile strength increase with increasing draw ratio analogously to the case of the 145 M sheet. There is however a notable difference between the tensile properties of the melt drawn 145 M and 240 M sheets. Although melt drawing is less effective for increasing the tensile properties of 145 M sheet, the Young's modulus and tensile strength of the 240 M sheet can be much improved by melt drawing. In fact, the Young's modulus of 240 M sheet obtained by melt drawing is higher than that by solid drawing. The tensile strength is more sensitive to drawing temperature than the Young's modulus. At a given draw ratio, the tensile strength of solid drawn 240 M sheet increases with the rise in drawing temperature, while the opposite trend is observed in melt drawn 240 M sheet.

Figs. 16 and 17 show the Young's modulus and tensile strength, respectively, of the 340 M sheet. The tensile properties of hot drawn 340 M sheet show similar tendencies to those of the 240 M sheet in the effects of draw ratio and drawing temperature. However, the maximum draw ratio for 340 M sheet is lower than that for the 240 M sheet. As a result, the highest Young's modulus obtained for 340 M sheet is lower than that of 240 M sheet.

In the course of melt drawing, the entangled molecular chains are aligned in the drawing direction. Accordingly, the tensile properties can be improved by melt drawing. In the case of 145 M with lower molecular weight, the disentanglement takes place more frequently in melt drawing process, which gives negative effect on the transmission of drawing stress and favors the mobility of molecular chains. Therefore, the melt drawing is less effective in the UHMWPE having lower molecular weight.
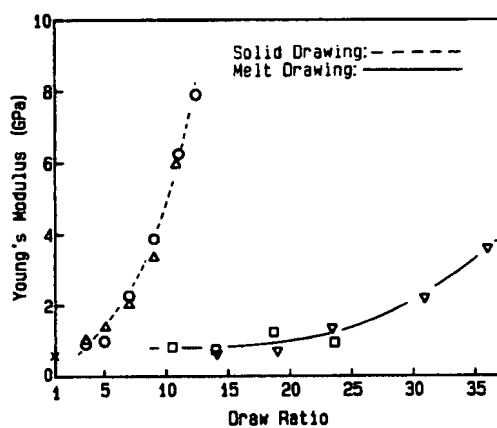
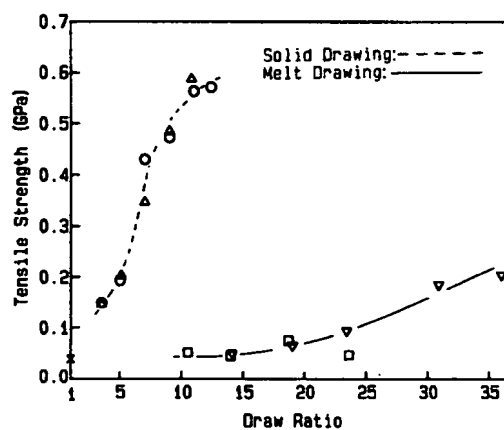Figure 12. Young's modulus vs.draw ratio for hot drawn 145 M sheets: △;120 °C, ○;130 °C, ▽;135 °C, □;140 °C

Figure 13. Tensile strength vs. draw ratio for hot drawn 145 M sheets: △;120 °C, ○;130 °C, ▽;135 °C, □;140 °C
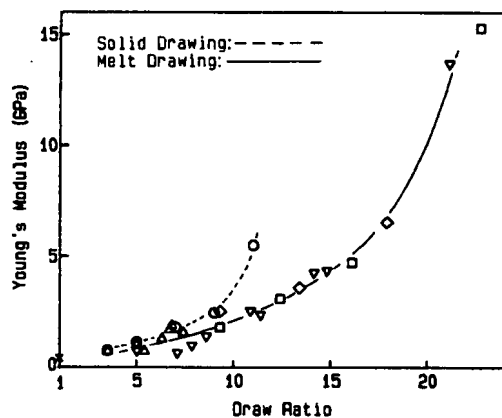
Figure 14. Young's modulus vs.draw ratio for hot drawn 240 M sheets: △;120 °C, ○;130 °C, ▽;135 °C, □;140 °C, ◇;150 °C.
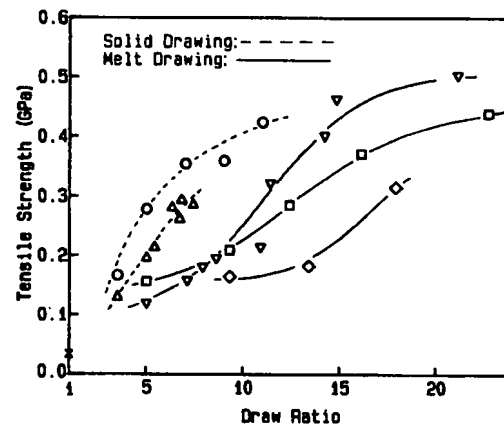
Figure 15. Tensile strength vs. draw ratio for hot drawn 240 M sheets: △;120 °C, ○;130 °C, ▽;135 °C, □;140 °C, ◇;150 °C.
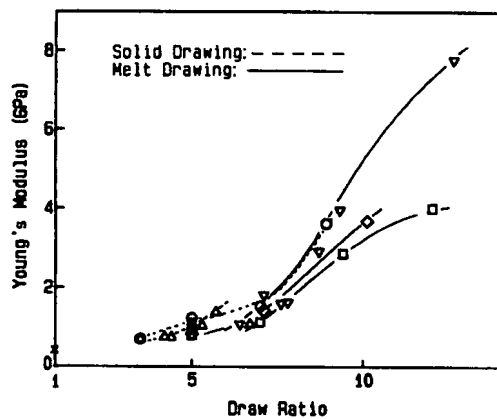
Figure 16. Young's modulus vs.draw ratio for hot drawn 340 M sheets: △;120 °C, ○;130 °C, ▽;135 °C, □;140 °C, ◇;150 °C.
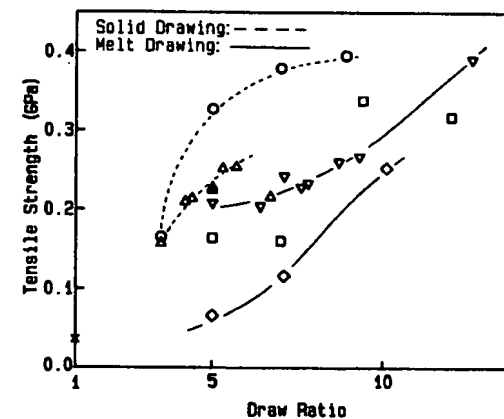
Figure 17. Tensile strength vs. draw ratio for hot drawn 340 M sheets: △;120 °C, ○;130 °C, ▽;135 °C, □;140 °C, ◇;150 °C.

STRUCTURE OF HOT DRAWN UHMWPE

The structure of hot drawn UHMWPE sheets was characterized by wide angle X-ray diffraction (WAXD), differential scanning calorimetry (DSC), and dynamic mechanical tests. Also, periodic layer structure was investigated by small angle X-ray scattering (SAXS).

The WAXD pole figure was obtained by Ni-filtered Cu Kα radiation. The WAXD intensity was measured by employing both Decker transmission method and Schultz reflection method, and then corrected for background and absorption of the specimens. The 200 and 020 pole figures of the melt drawn UHMWPE sheets are shown in Fig. 18. The principal axes of the sheets are labeled M (draw direction), T (transverse direction), and N (normal direction). The 200 and 020 pole densities are distributed in the T - N plane, suggesting that the crystal c-axis orients to the draw direction (M). The b-axis tends to be aligned to the transverse direction, whereas the 200 pole maxima are inclined from the normal direction by 5-15°. The doubly oriented texture might be originated from the kink of crystals.
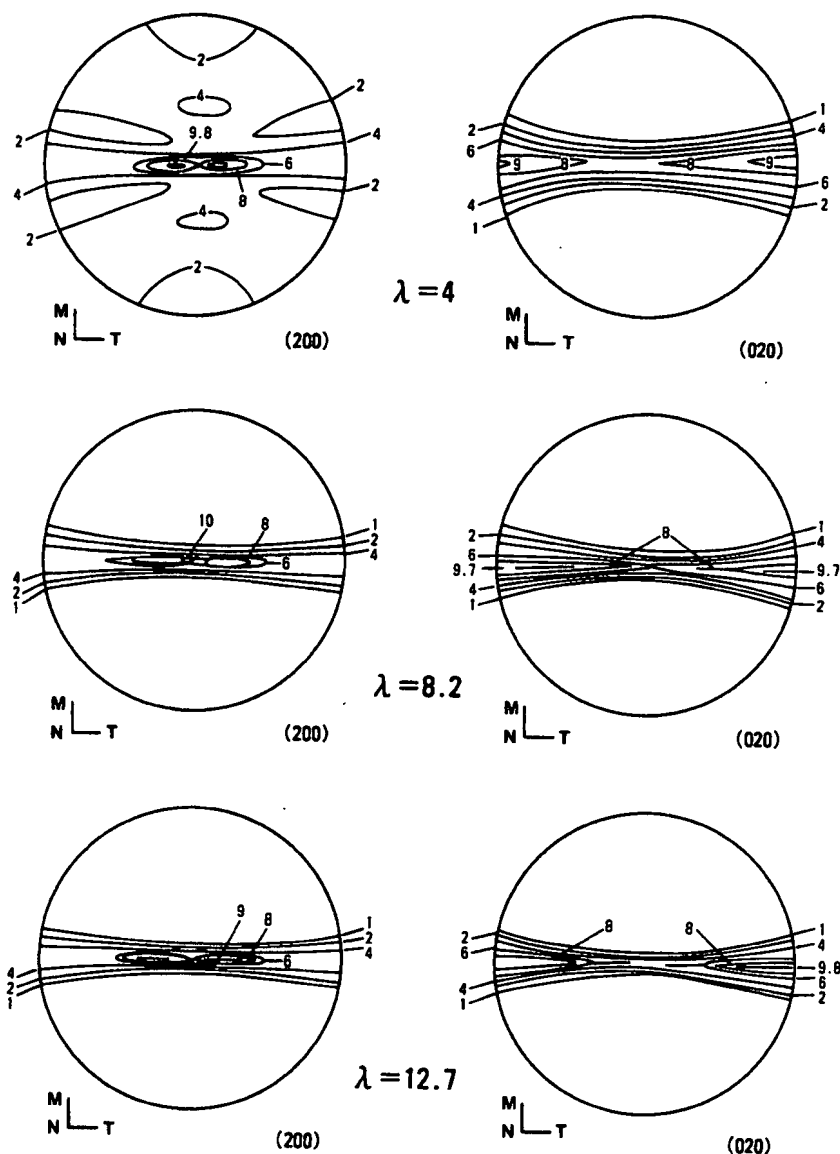

Figure 18. Change of 200 and 020 pole figures of hot drawn 240 M sheets with draw ratios: Drawing temperature, 140 °C.
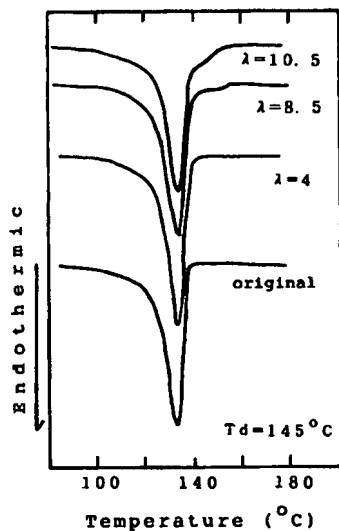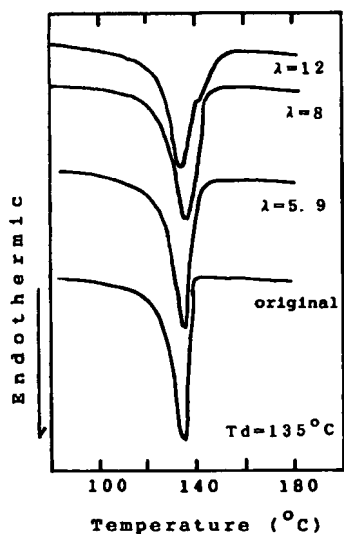
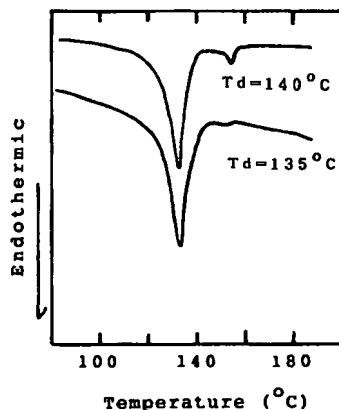Figure 19. DSC curves of 240 M sheets melt drawn in one stage.

Figure 20. DSC curves of 240 M sheets melt drawn in two stages.

The texture of the sample with lower draw ratio is more complex. The 200 pole figure consists of high maxima on the equator and a small peak at 40 - 45 ° from draw direction to normal direction. The result shows the presence of two modes of orientation of the a-axis: one highly oriented perpendicularly to the draw direction and another weakly oriented between normal direction and draw direction.

The DSC measurements were carried out under a nitrogen atmosphere at a heating rate of 10 K/min. The DSC curves of the melt drawn 240 M sheets are shown in Fig. 19. The temperature at the end of crystal melting shifts to the higher temperature region with increasing draw ratio and a shoulder peak appears on the higher temperature side of the main peak at draw ratios higher than 6. The appearance of the higher melting peak is originated from the extension of molecular chains and the formation of extended chain crystals.

Fig. 20 shows the DSC curves for the 240 M sheets which are melt drawn in two stages. Besides a main peak, a small melting peak is observed at 152 - 153 °C, suggesting that a small amount of orthorhombic extended chain crystals are produced by the two-stage drawing in the melt state.

Keller et al. proposed a model for the stress-induced crystallization of crosslinked polyethylene (ref. 9,10). The structure development in the melt-drawn UHMWPE sheets can be explained by this model. It is likely that a few extended chain crystals are formed at the initial stage of stretching and act as nucleation centers for the succeeding crystallization process. The crystals grow from the nucleation center, which is aligned to the drawing direction. At high stress (high draw ratio), the crystal grow in a column with the c-axis parallel to the draw direction. On the other hand, at low stress, the crystals grow in the radial direction as in the normal spherulites, without retaining molecular orientation. Both textures are formed at lower draw ratio, giving rise to the bimodal orientation of the a-axis.

The SAXS patterns of the hot drawn sheets were taken with a vacuum camera using a pinhole beam of Ni-filtered Cu Kα radiation. Tsvankin et al. theoretically analyzed the various type of SAXS patterns (ref. 11). Fig. 21 shows the SAXS patterns of the 240 M sheet. The solid drawn sheet shows a four-point pattern which is attributed to a stacking of

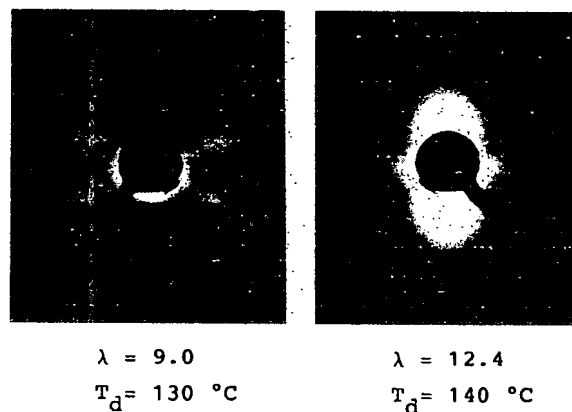λ = 9.0   λ = 12.4

T_d = 130 °C T_d = 140 °C

Figure 21. SAXS patterns of 240 M sheets.

inclined periodic layers. The periodic layer is formed by the arrangement of crystallites with the molecular chains parallel to the draw direction. On the other hand, the SAXS pattern of the melt drawn sheet is characterized by a two-point pattern on the meridian. The normals of the periodic layers are aligned parallel to the draw direction in the melt drawn UHMWPE sheet.

The crystallite size along the molecular chain axis (c-axis), D_{002}, was calculated from the broadening of the (002) reflection by using Scherrer's equation. The profiles obtained for the drawn sheets were corrected for instrumental broadening and the $K\alpha$ doublet. Silicon single crystal was used as standard. Crystallite size, D_{002}, long period d, and lattice distortion ε, for the drawn sheets of UHMWPE are shown in Table 5. The D_{002} approaches the d in the two-stage drawn sheets. This means that amorphous region between lamellae decreases, and that extended chain crystals are produced and pass through amorphous region. Gibson et al. reported that the crystalline bridges were formed between crystallites in the hot drawn HDPE sheets (ref. 12). As obvious from Table 5, crystallite size along c-axis increases considerably and long period remains fairly constant with increasing draw ratio. Both D_{002} and d decrease in the two-stage drawn sheets. This may be due to smaller draw ratio in the second stage drawing and there are two recrystallization processes: relaxed chains in the melt form folded chain crystals and unrelaxed chains develop extended chain crystals.

Dynamic mechanical behaviors for the drawn sheets reflect also structure characteristics. Fig. 22 indicates that β-relaxation appears in the lower draw ratio sheets. β-relaxation intensity increases due to loosening of network structure formed by entanglement in initial stage of deformation. We suggest that β-relaxation of the drawn sheets of UHMWPE is due to chain segment activities in amorphous region composed of entangled molecules. In higher draw ratio or two-stage drawn sheets, larger size crystals are produced and pass through the amorphous region and thus the amorphous segment activities may decline, so that β-relaxation degenerates greatly or disappears.

TABLE 5. Crystallite size, long period, and lattice distortion of UHMWPE sheets drawn at 140°C

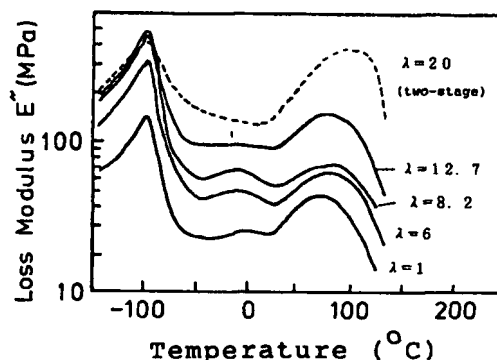| Draw ratio	$D_{002}(\overset{\circ}{A})$	$d(\overset{\circ}{A})$	$\varepsilon(\%)$
6	323	414	0.36
8.1	355	401	0.37
11	362	410	0.11
22*	340	352	0.25

*: Two-stage drawing (11 × 2)

Figure 22. Dynamic mechanical behaviors of UHMWPE sheets drawn at 140 °C:
Draw Ratio, A;1, B;6, C;8.2, D;12.7, E;20 (two-stage drawing).

REFERENCES

1. R. Chiang, J. Polym. Sci., 36, 3 (1959).
2. P. M. Henry, J. Polym. Sci., 36, 91 (1959).
3. R. W. Truss, K. S. Han, J. F. Wallence, and P. H. Geil, Polym. Eng. Sci., 20, 747 (1980).

4. G. W. Halldin and I. L. Kamel, Polym. Eng. Sci., 17, 21 (1977).
5. G. Capaccio and I. M. Ward, Polymer, 16, 239 (1975).
6. G. Capaccio, T. A. Crompton, and I. M. Ward, J. Polym. Sci., Polym. Phys. Ed., 18, 1301 (1980).
7. L. R. G. Treloar, The Physics of Rubber Elasticity, 3rd Ed., Clarendon, Oxford, 1975.
8. P. Smith, P. J. Lemstra, and H. C. Booij, J. Polym. Sci., Polym. Phys. Ed., 19, 877 (1981).
9. A. Keller and M. J. Marchin, J. Macromol. Sci., B, 1, 41 (1967).
10. M. J. Hill and A. Keller, J. Macromol. Sci., B, 3, 153 (1969).
11. V. I. Gerasimov, Ya V. Genin, and D. Ya Tsvankin, J. Polym. Sci., Polym. Phys. Ed., 12, 2035 (1974).
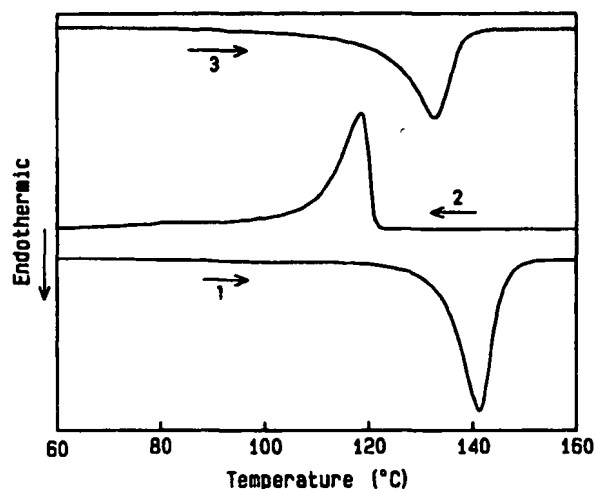12. A. G. Gibson, G. R. Davies, and I. M. Ward, Polymer, 19, 683 (1978).

Figure 2. DSC curves for
UHMWPE 240 M powder:
1;first heating process,
2;cooling process,
3;second heating process.

TABLE 2. Melting and crystallization temperatures of UHMWPE powder
samples

Powder	First scanning						Second scanning		
	T_{im}	T_{pm}	T_{em}	T_{ic}	T_{pc}	T_{ec}	T_{im}	T_{pm}	T_{em}
					(°C)				
145 M	130.7	140.2	147.5	118.9	116.7	107.7	121.7	132.9	139.4
240 M	132.8	141.2	146.3	120.6	118.2	108.2	120.6	132.9	138.1
340 M	135.0	143.1	148.1	121.9	119.1	109.9	125.2	134.4	139.2

T_{im} : extrapolated onset temperature of melting
T_{pm} : melting peak temperature
T_{em} : extrapolated end temperature of melting
T_{ic} : extrapolated onset temperature of crystallization
T_{pc} : crystallization peak temperature
T_{ec} : extrapolated end temperature of crystallization

PROPERTIES-MOLECULAR WEIGHT RELATIONSHIPS

Chemically, UHMWPE is identical with HDPE. In general, the molecular weight strongly influ-
ences on physical properties of polymers. Attempts have been made to deal with the rela-
tionships between physical properties and molecular weights of UHMWPE.

Preparation of specimen

The sheets of thickness 1 - 3 mm were
prepared by compression molding of UHMWPE
powders with a cylindrical type mold. The
molding procedures to get homogeneous and
uniform specimens are shown in Table 3.
The powder was placed in the mold, heated
and kept under a pressure of 10 MPa.
Pressure applied on the melt was then
decreased to 5 MPa. After the dwell-time
of 20 minutes, the sample was cooled, kept
at 20 - 30 °C under a pressure of 20 MPa
and then taken out of the mold.

TABLE 3 Condition for compression molding
of UHMWPE

Step	Temperature (°C)	Pressure (MPa)	Hold time (min)
1st	200 - 220	10	5
2nd	200 - 220	5	15
3rd	20 - 30	5	0.5
4th	20 - 30	20	20

Characterization of Polyethylene with Differential Scanning Calorimetry (DSC) and Dynamic Mechanical Analysis (DMA)

Introduction

Polyethylene (PE) is a generally semi-crystalline thermoplastic material which is frequently used for consumer products such as foils (wrapping, packaging), containers (bottles, tanks), pipes, tubes or other engineered products. PE is odorless, flavorless and physiologically indifferent and can therefore be used in the food industry (1).

PE is classified in the following categories:

UHMWPE	(ultrahigh molecular weight PE)
HDPE	(high density PE)
LDPE	(low density PE)
LLDPE	(linear low density PE)

The mechanical and thermal properties of PE significantly depend on the crystal structure, crystallinity degree, molecular weight and branching. The temperatures of the melting range and glass transition point vary strongly with the PE type (2).

Instrumentation and Methods

Differential Scanning Calorimetry (DSC)

DSC instruments are widely used for the thermal characterization of polymers (3). For practical applications, the interest is mostly focused on the glass transition temperature, melting range and heat of fusion (crystallinity), curing behavior and decomposition of the material. Most of the DSCs are also able to determine the specific heat (c_p) of the material (specimen).

There are two types of DSC instruments: power compensated and heat flux DSCs. The most commonly used DSC type in analytical laboratories is based on the heat flux principle. The construction principle of a typical heat flux DSC (NETZSCH DSC 204 *F1 Phoenix*®) is shown in figure 1. The sample pan and the generally empty reference pan are located in a furnace and heated or cooled by a controlled temperature program. As long as the sample and the reference material respond to the temperature program in the same way, the heat flux into the sample and the reference remains nearly constant. This means that the temperature difference between the two sensor plates remains nearly constant. If the sample "absorbs" heat because of melting or a glass transition, a difference in the heat flux occurs and an endothermal effect is detected in the DSC curve. During crystallization or curing, energy is released by the sample and an exothermal DSC effect is observed. Calibration of the DSC by a sensitivity curve is required to determine the heat flow from the measured temperature difference (difference in thermocouple voltage). Integration of the resulting heat-flow curve yields quantitative values for enthalpy changes. Heat flux DSCs are robust, easy-to-handle and feature a stable and reproducible baseline.
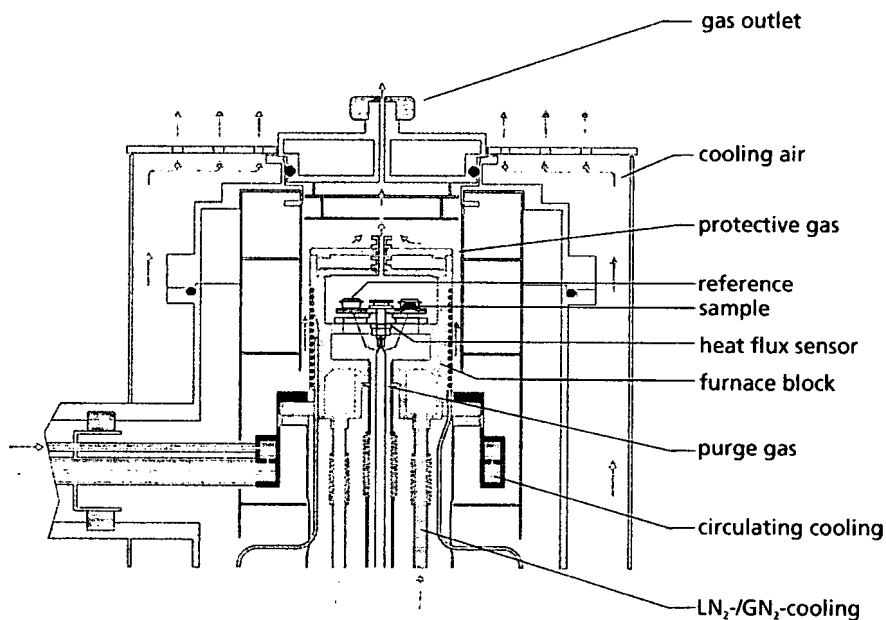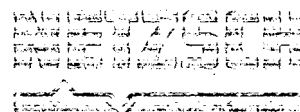

Figure 1. Scheme of a heat flux DSC (DSC 204 F1 *Phoenix*®)

Oxidative Induction Time/Temperature (OIT)

OIT tests can be performed with DSC instruments by comparing the thermal stability of materials to thermo oxidative attack. There are two measurement methods:

Dynamic OIT method: the sample is heated in air or oxygen at a linear heating rate. The characteristic temperature of the beginning of the oxidation process is determined by analyzing a shift from the baseline due to exothermic oxidation reactions.

Static OIT method: the sample is heated in an inert gas atmosphere over the melting point to the selected test temperature. The temperature is then kept constant. After reaching an equilibrium, the gas is switched to air or oxygen. The oxidative reaction normally occurs after a certain time period.

Dynamic OIT is faster but less sensitive. It works for almost all polymers. Static OIT is more sensitive but also more time-consuming. The static method is normally used for quality control of polyolefin-based polymers because it is standardized. (DS 2131.2, ASTM D3895, ISO 11357-6).

Dynamic Mechanical Analysis (DMA)

Dynamic mechanical analysis (DMA) yields information about the mechanical and viscoelastic properties of a sample as a function of time and temperature by applying an oscillating force. Depending on the stiffness and damping behavior, the response of the sample on the external load differs in amplitude and phase shift. The mathematical and physical relation of the characteristic curves and values (complex modulus E^*, storage modulus E', loss modulus E'' and loss factor tan δ) are described in ISO 6721-1.

Basically, there are two types of DMA measurements:

- deformation controlled – applies a sinusoidal deformation to the sample and measures the stress

- force controlled – applies a sinusoidal stress and measures deformation

Depending on the available sample size, sample behavior etc. different measurement setups (e.g. 3-point bending) can be applied. Figure 2 shows the scheme of the NETZSCH DMA 242. Some available sample holders for the different measurement modes are depicted in figure 3.

force (up to 16 N)

oscillator — — force signal

— automatic adjustment

displacement sensor — → displacement signal

pushrod —

sample —
max. length 60 mm)

stepper motor
(adjustment control)

sample thermocouple

sample holder
3 point bending
(single/dual cantilever
compression/penetration,
shearing, tension)

control thermocouple

rectangular furnace
(homogeneity +/- 1°C)

cooling device
(20°C ... –150°C in 10 min)

sample displacement
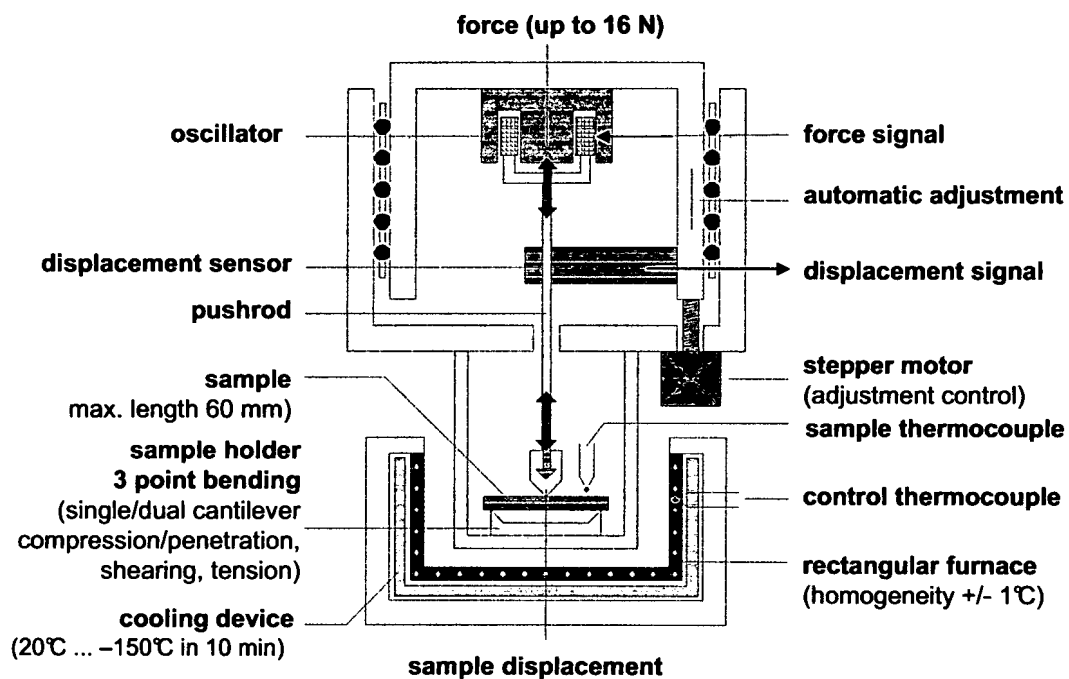
Figure 2. Scheme of the NETZSCH DMA 242

✓ Single / Dual Cantilever

✓ Shear

✓ Compression/
Penetration

Prestress
(Static)

Oscillation

Sample

✓ 3-Point Bending

✓ Tension
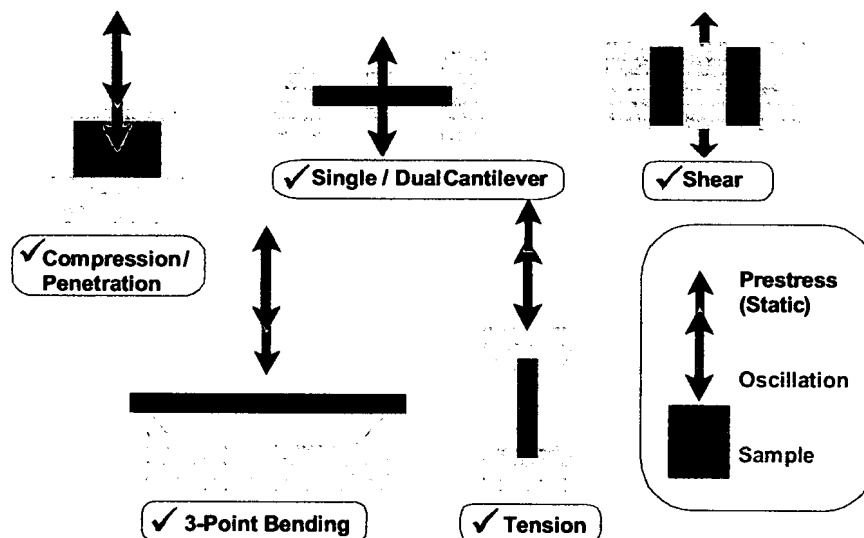
Figure 3. DMA measurement modes

Experimental

The DSC measurements were performed with the NETZSCH DSC 200 *F3 Maia*®. The samples were heated twice at a heating rate of 10 K/min from RT to 160°C and −150 to 160°C. Between the two heating segments, a controlled cooling at 20 K/min was applied. The sample weights were between 8 and 9 mg. The samples were contained in Al pans with pierced lids. The atmosphere was N_2 with a flow rate of 20 ml/min. The OIT tests were performed using the static method. The samples were heated in N_2 to 200°C at 10 K/min, then held isothermal for 2 min in an N_2 atmosphere at this temperature. After this equilibration time, the gas atmosphere was switched to oxygen. For these measurements, Al pans with pierced lids (3 holes) were employed. The sample weight was approx 1.4 mg each.

The DMA measurements were conducted with a NETZSCH DMA 242. The sample (granulate grain) was measured in the compression mode at a heating rate of 2 K/min in an N_2 atmosphere. An oscillation frequency of 1 Hz was applied.

Results

The heat flow rate curves of LDPE during the first and second heating are shown in figure 4. During the first heating, the sample shows some memory effects at about 90°C from the production process. During the second heating run, these effects are removed because of the previous controlled cooling. The melting temperature is approx. 114°C (peak temperature) which is at the upper limit for LDPE. For characterization of the melting range of polymers, the peak temperature is usually used.

The melting behavior of LLDPE is plotted in figure 5. Again, during the first heating, influences of the thermal history are visible. The melting temperature (approx. 127°C) is in the typical melting range for LLDPE, but also at the higher end.
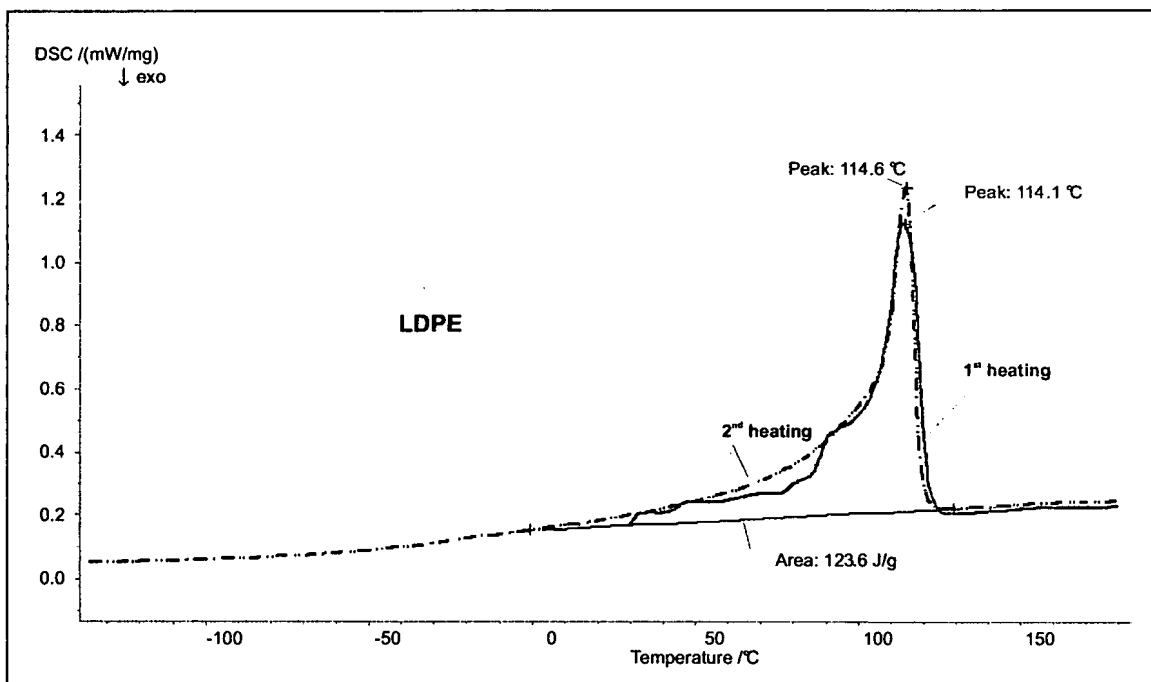
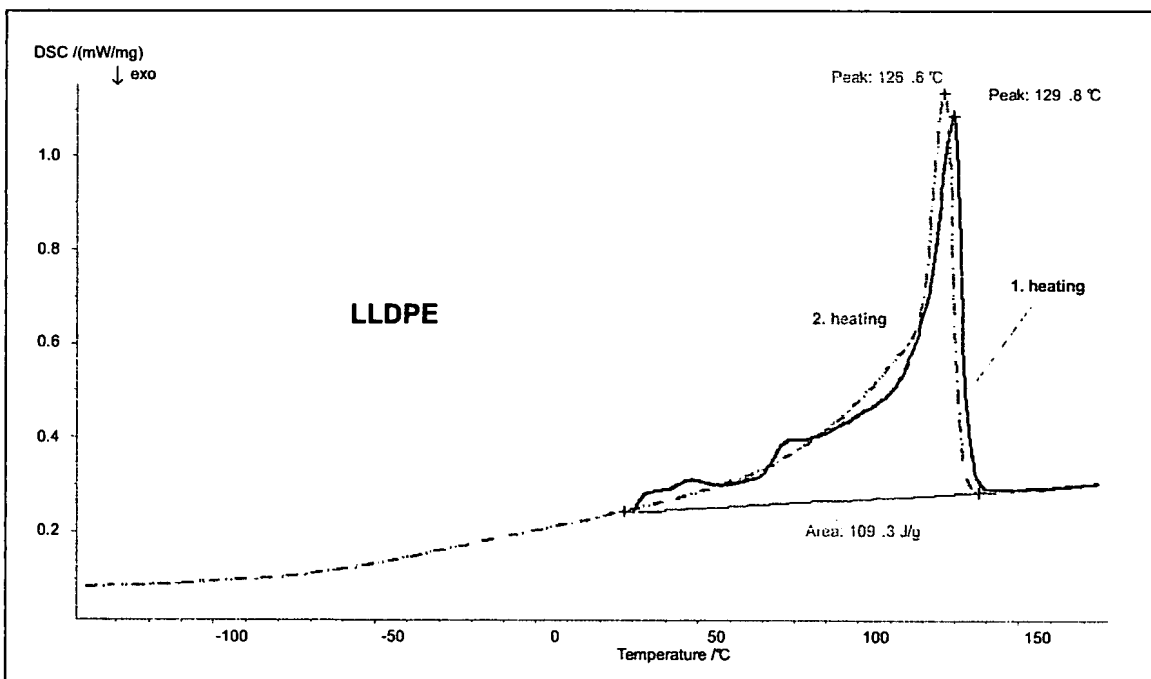**Figure 4. DSC curves of LDPE (1st and 2nd heating)**

Figure 5. DSC curves LLDPE (1st and 2nd heating)

HDPE melts at the highest temperature of the 3 samples (figure 6). The peak temperature was at approx. 137°C, which is in the typical range for HDPE materials. A comparison of the melting of the 3 PE types is shown in figure 7. The differences in the melting behavior of the different PE types analyzed are clearly visible.
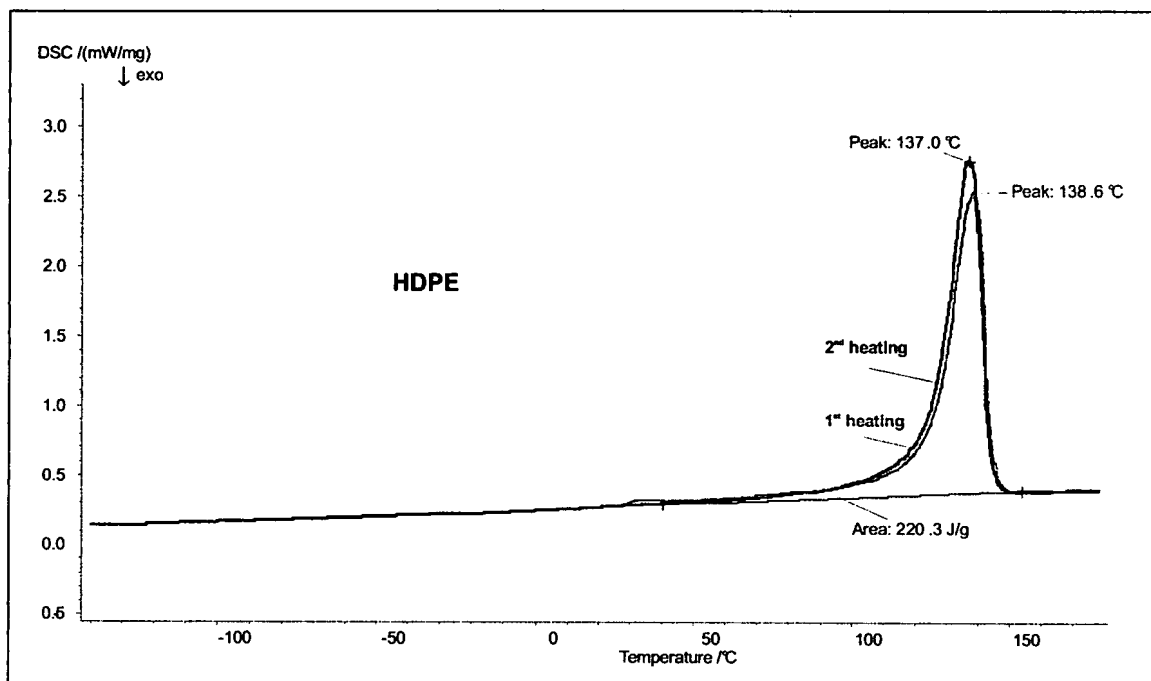

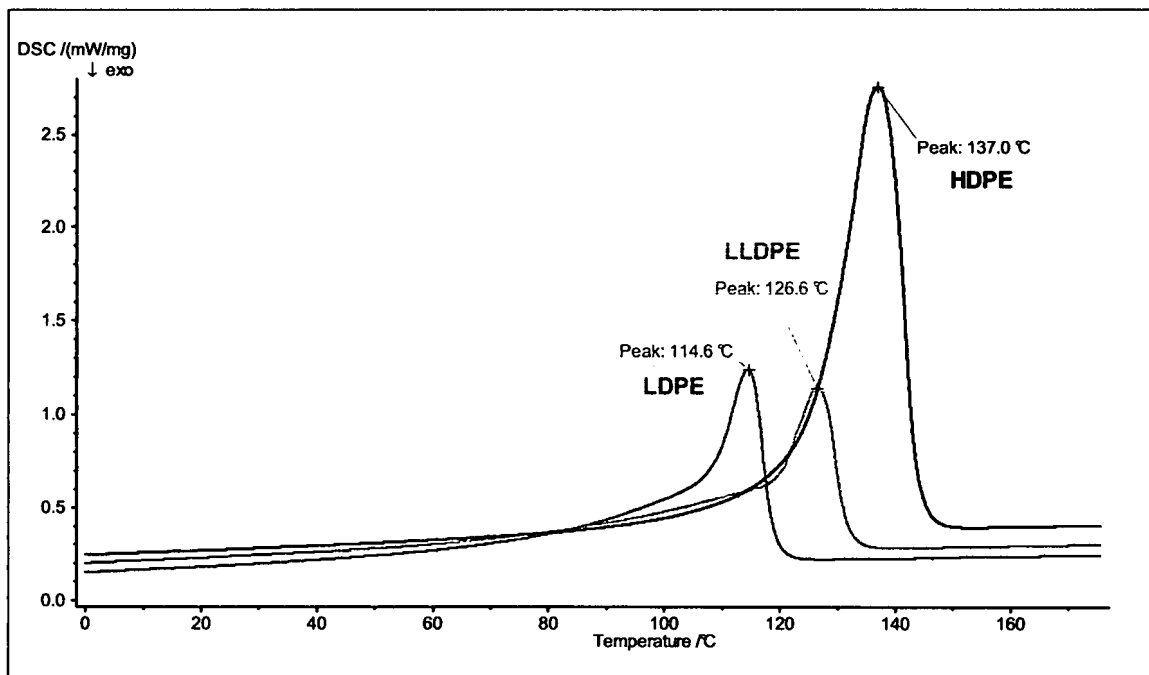**Figure 6. DSC curves of HDPE (1ˢᵗ and 2ⁿᵈ heating)**

Figure 7. Comparison of the melting of LDPE, LLDPE and HDPE.

Due to the extremely small change in the specific heat, it is often very hard to detect the glass transition of PE. In figure 8, an example of the glass transitions of two HDPE samples is shown. The delta c_p value of 0.01 J/g of these samples is small and generally below the detection limit of most DSC instruments. For such small glass transitions, the DMA offers a higher sensitivity. In figure 9, the DMA results for an HDPE sample are evaluated. The peak temperatures of tan delta and the loss modulus E″ are in good agreement with the DSC midpoint. In general, the peak temperature of the loss modulus (E″) curve at a frequency of 1 Hz is used as the glass transition temperature (Tg). In the DSC, the midpoint of the step is evaluated as Tg.
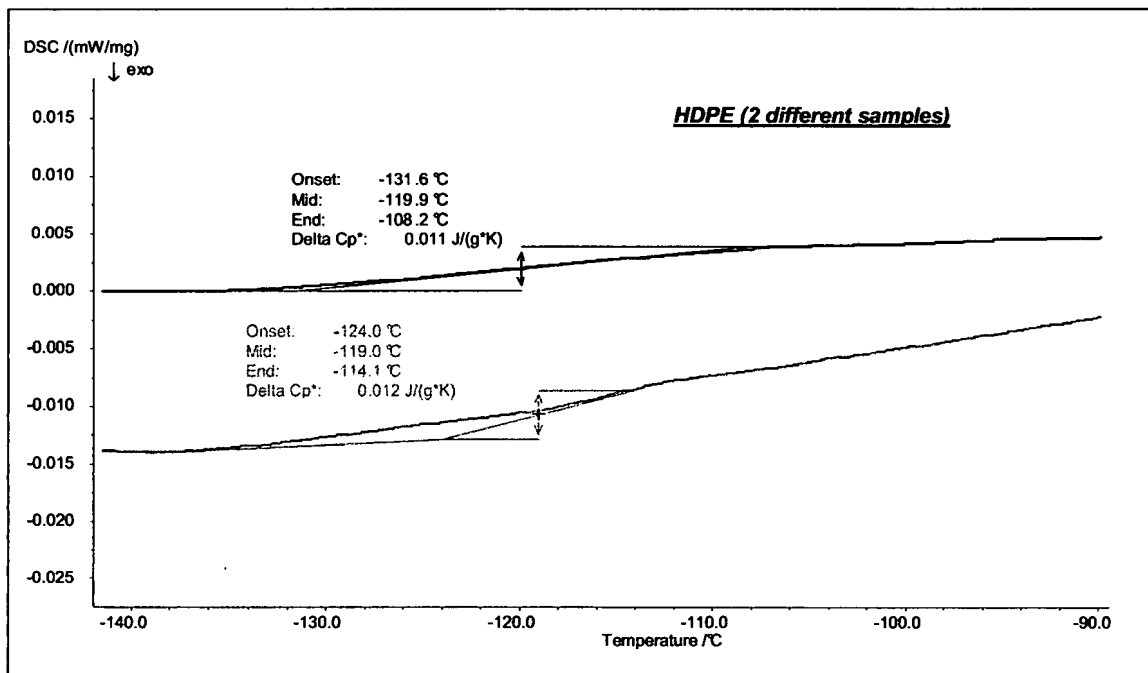
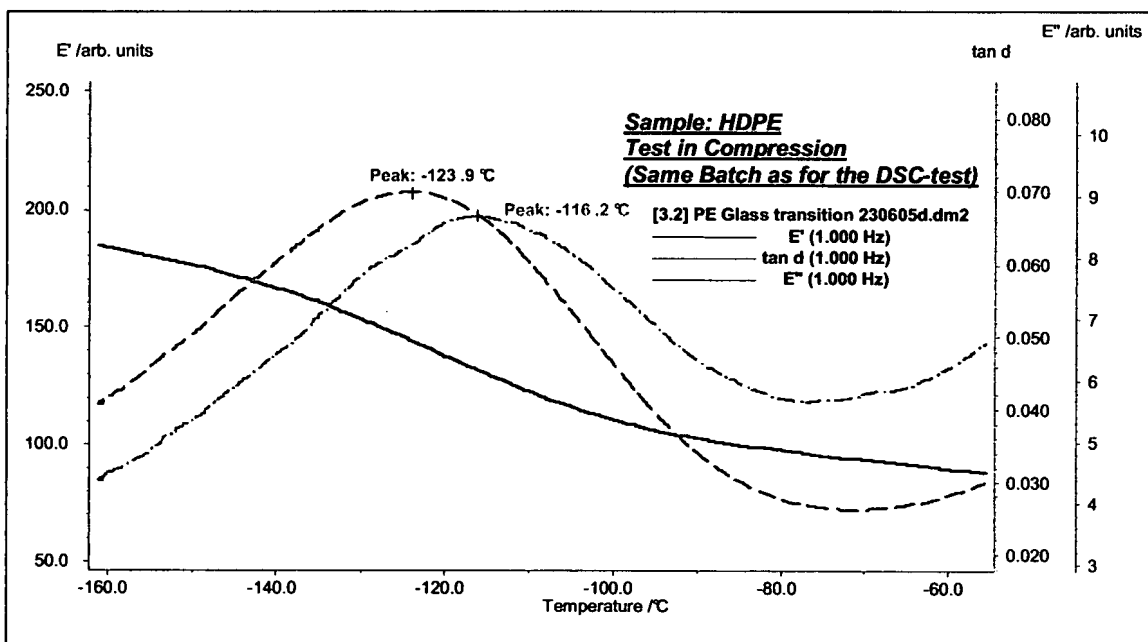**Figure 8. Evaluation of the glass transition of 2 different HDPE samples measured with DSC**

Figure 9. Glass transition of HDPE measured with the DMA

The OIT results for two different PE films are compared in figures 10 and 11. As can be seen from figure 10, one sample is a pure PE sample (peak temperature 109.8℃, most probably LDPE). The second sample is a blend of different PE types. The thermal degradation of the PE1 sample starts earlier (extrapolated onset) than the blend. This means that the blend is slightly more resistant to oxidative attack.
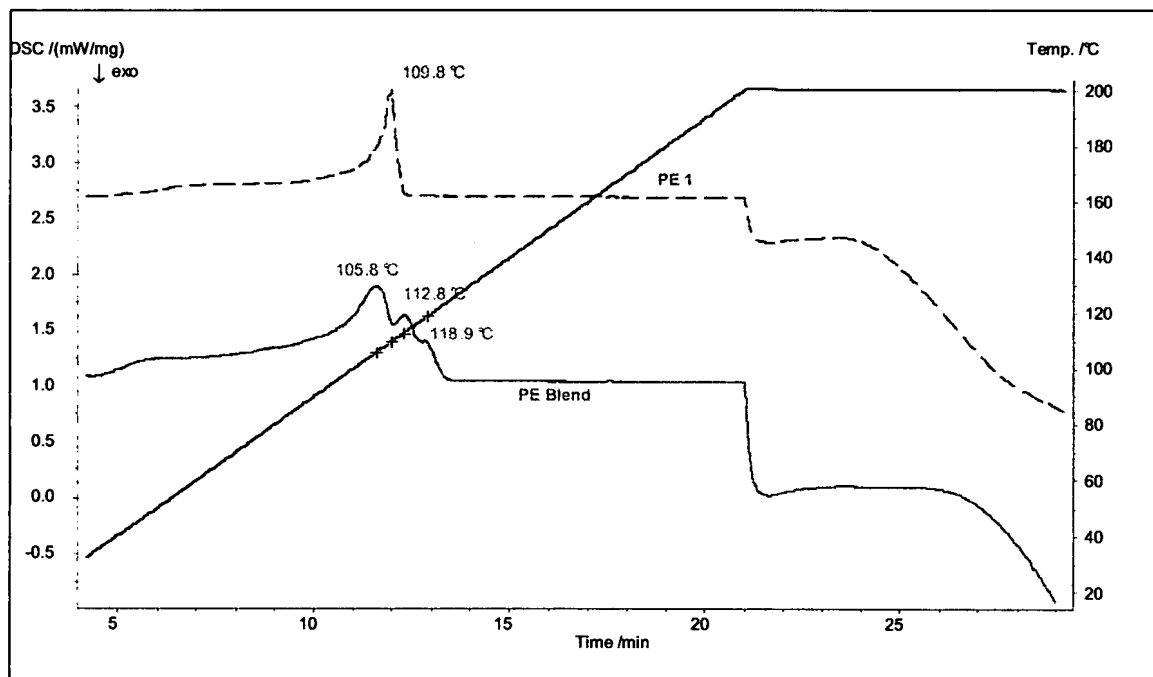

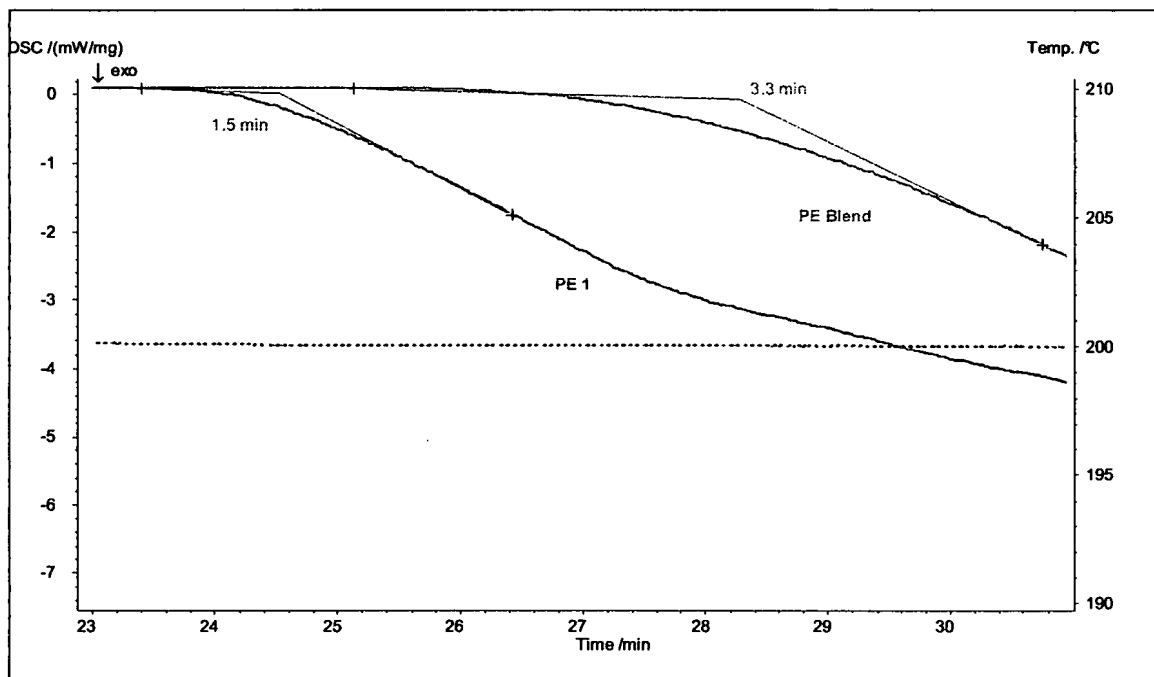**Figure 10. OIT measurements of 2 different PE samples**

Figure 11. OIT results for 2 PE foils

Conclusion

DSC delivers information on the melting temperature of PE which can be used for distinction of the different PE types. The glass transition temperature of PE is only a weak step in the DSC curve but can easily be detected with the DMA. With OIT tests employing the DSC, a comparison of the thermal stability of the different samples can be carried out. Aging effects or presence and effectiveness of stabilizers can also be analyzed with the OIT method.

Literature

(1)   Saechtling, Kunststofftaschenbuch, Carl Hanser Verlag, München Wien 1998

(2)   TA für die Polymertechnik, NETZSCH Jahrbuch für Wissenschaft und Praxis, Band 2

(3)   Thermal Analysis of Plastics, G. Ehrenstein, G. Riedel, P. Trawiel, Carl Hanser Verlag Munich 2004